A catalytic function for the structurally conserved residue Phe 100 of ribonuclease T 1

ARTICLE *in* PROTEIN SCIENCE · AUGUST 1996

Impact Factor: 2.85 · DOI: 10.1002/pro.5560050808 · Source: PubMed

6 AUTHORS, INCLUDING:

Ingrid Zegers
European Commission
60 PUBLICATIONS **960** CITATIONS
SEE PROFILE

Remy Loris
Vrije Universiteit Brussel
150 PUBLICATIONS **4,148** CITATIONS
SEE PROFILE

Lode Wyns
Vrije Universiteit Brussel
269 PUBLICATIONS **9,679** CITATIONS
SEE PROFILE

Jan Steyaert
Vrije Universiteit Brussel
136 PUBLICATIONS **4,687** CITATIONS
SEE PROFILE

Protein Science (1996), 5:1523–1530. Cambridge University Press. Printed in the USA.

A catalytic function for the structurally conserved residue Phe 100 of ribonuclease T_1

JAN DOUMEN,[1] MALGORZATA GONCIARZ,[1,2] INGRID ZEGERS,[1] REMY LORIS,[1] LODE WYNS,[1] AND JAN STEYAERT[1]

[1] Dienst Ultrastructuur, Vlaams Interuniversitair Instituut Biotechnologie, Vrije Universiteit Brussel, Paardenstraat 65, B-1640 Sint-Genesius-Rode, Belgium

(RECEIVED January 22, 1996; ACCEPTED May 21, 1996)

Abstract

The function of the conserved Phe 100 residue of RNase T_1 (EC 3.1.27.3) has been investigated by site-directed mutagenesis and X-ray crystallography. Replacement of Phe 100 by alanine results in a mutant enzyme with k_{cat} reduced 75-fold and a small increase in K_m for the dinucleoside phosphate substrate GpC. The Phe 100 Ala substitution has similar effects on the turnover rates of GpC and its minimal analogue GpOMe, in which the leaving cytidine is replaced by methanol. The contribution to catalysis is independent of the nature of the leaving group, indicating that Phe 100 belongs to the primary site. The contribution of Phe 100 to catalysis may result from a direct van der Waals contact between its aromatic ring and the phosphate moiety of the substrate. Phe 100 may also contribute to the positioning of the pentacovalent phosphorus of the transition state, relative to other catalytic residues. If compared to the corresponding wild-type data, the structural implications of the mutation in the present crystal structure of Phe 100 Ala RNase T_1 complexed with the specific inhibitor 2′-GMP are restricted to the active site. Repositioning of 2′-GMP, caused by the Phe 100 Ala mutation, generates new or improved contacts of the phosphate moiety with Arg 77 and His 92. In contrast, interactions with the Glu 58 carboxylate appear to be weakened. The effects of the His 92 Gln and Phe 100 Ala mutations on GpC turnover are additive in the corresponding double mutant, indicating that the contribution of Phe 100 to catalysis is independent of the catalytic acid His 92. The present results lead to the conclusion that apolar residues may contribute considerably to catalyze conversions of charged molecules to charged products, involving even more polar transition states.

Keywords: enzyme mechanism; functional cooperativity; RNase T_1; site-directed mutagenesis; subsite binding

RNase T_1 (EC 3.1.27.3) from the fungus *Aspergillus oryzae* is the best known representative of a large family of homologous microbial ribonucleases (Hill et al., 1983). The enzyme cleaves the P-O5′ ester bond of GpN sequences of single-stranded RNA by a transesterification reaction, yielding a 2′,3′-cyclic phosphate. The associative nucleophilic displacement at the phosphorus atom of the 5′-leaving group by the entering 2′-oxygen is thought to follow a concerted in line mechanism, with a trigonal bipyramidal transition state, implying a base and an acid located on either side of the scissile bond (Eckstein et al., 1972). The active site geometry, early biochemical data, and the kinetic effects of single mutations are in full agreement with the widely accepted view that Glu 58 and His 92 serve as base and acid catalyst, respectively (Heinemann & Saenger, 1982; Steyaert et al., 1990). Tyr 38, His 40, and Arg 77 contribute to the stabilization of the transition state of the transesterification reaction (Nishikawa et al., 1987; Arni et al., 1988; Steyaert et al., 1990, 1991a; Grunert et al., 1991). The subsite residues Asn 36 and Asn 98 accelerate the chemical turnover of GpN dinucleoside phosphate substrates through interactions with the leaving nucleoside N (Steyaert et al., 1991a).

Structural conservation of particular enzyme residues among homologous family members is indicative of their structural or functional importance (Poteete et al., 1992). Glu 58, Arg 77, and His 92 are indeed strictly conserved among all microbial ribonucleases. Tyr 38 and His 40 are conserved among the fungal ribonucleases (Hill et al., 1983). So far, another conserved residue (Phe 100) that is present in the active site of RNase T_1 has escaped attention. This phenylalanine has been found in all known

Reprint requests to: J. Steyaert, Dienst Ultrastructuur, Vlaams Interuniversitair Instituut Biotechnologie, Vrije Universiteit Brussel, Paardenstraat 65, B-1640 Sint-Genesius-Rode, Belgium; e-mail: jsteyaer@vub.ac.be.

[2] Present address: Institute of Biochemistry, University of Wroclaw, Tamka 2, 50-137 Wroclaw, Poland.

Abbreviations: 3′-CMP, 3′-cytidylic acid; 2′-GMP, 2′-guanylic acid; 3′-GMP, 3′-guanylic acid; 2′,5′-GpG, guanyl-2′,5′-guanosine; GpOMe, guanosine-3′-(methyl phosphate); MPD, 2-methyl-2,4-pentanediol; NpN, 3′,5′,-linked dinucleoside monophosphate compounds (N represents any of the four common nucleosides); RNase T_1, Ribonuclease T_1.

fungal members; a structurally equivalent tyrosine (Tyr 103; barnase numbering) is present in the bacterial enzymes. In the case of barnase, the Tyr 103 Phe mutant has been characterized kinetically (Meiering et al., 1992). It has been shown that the hydroxyl group of Tyr 103 does not contribute to dinucleoside phosphate turnover; only minor effects were observed on K_m. These data suggest that, if the conserved Phe/Tyr residue has any functional importance, the aromatic ring is the critical feature of this residue. Therefore, we analyzed the functional role of the Phe 100 aromatic ring in RNase T_1. Here, we present kinetic and structural data of Phe 100 Ala RNase T_1 (see Kinemage 1). Our results show that the Phe 100 side chain is a primary site residue that contributes considerably to chemical turnover. Its possible catalytic function is discussed below.

Results and discussion

Phe 100 contributes to substrate turnover at the primary site

Site-directed mutagenesis is a powerful tool to analyze the function of individual amino acids. The interaction energy of an individual side chain with the substrate may be analyzed by comparing the kinetics of wild-type enzyme with those for a mutant in which the side chain has been truncated; an apparent interaction energy is obtained (Fersht, 1988). The apparent binding energy is a measure of the specificity of binding or catalysis. In the present study, we compared the steady-state kinetic parameters of Phe 100 Ala RNase T_1 for the transesterification of the model substrate GpC with those of wild-type enzyme (Table 1). The Phe 100 to Ala replacement results in a considerable decrease in k_{cat} concomitant with only minor changes in the equilibrium dissociation constant (K_s) for the substrate, indicating that the Phe 100 phenyl group contributes to chemical turnover rather than to ground-state binding of the substrate. Apparently, the Phe 100 side chain contributes 2.6 kcal/mol to turnover and 1.0 kcal/mol to substrate binding.

For RNase T_1, subsite interactions with the leaving nucleoside N of GpN substrates make a considerable contribution to chemical turnover (Steyaert et al., 1991a). To analyze the interactions of Phe 100 with the leaving group, we measured the transesterification kinetics of Phe 100 Ala RNase T_1 for GpOMe, a synthetic minimal substrate in which the leaving nucleoside has been replaced by methanol (Table 1). The kinetics of wild-type and Phe 100 Ala RNase T_1 for the substrates GpC and GpOMe may be combined in a thermodynamic cycle (Fig. 1) to measure the energetics of the interactions between the Phe 100 side chain and the leaving group cytidine (Steyaert et al., 1991a). The degree to which the Phe 100 Ala mutation differentially affects the transesterification rates of GpC and GpOMe ($\Delta\Delta G$) measures the apparent interaction energy between the aromatic ring of Phe 100 and the leaving nucleoside cytidine. The effect of the Phe 100 Ala mutation on substrate turnover ($\Delta\Delta G_{cat}$) is independent of the presence of the leaving nucleoside cytidine, indicating that the Phe 100 side chain is contained in the primary site, rather than in the subsite of RNase T_1. In contrast, the contribution of Phe 100 to substrate binding appears to depend on the presence of the leaving nucleoside cytidine.

Structural implications of the Phe 100 Ala mutation

Detailed analysis of any protein engineering experiment is aided by high-resolution structural information. Because the Phe 100 side chain is buried in the RNase T_1 fold and makes direct contact with the side chain of His 92 in wild-type enzyme (Arni et al., 1988), we were concerned that the Phe 100 Ala mutation could exert an indirect damaging effect on turnover by inducing major changes in the overall structure of the primary site. Therefore, we examined the structural implications of the Phe 100 Ala mutation by X-ray crystallography (Table 2 and Kinemage 1). The structure of the complex between Phe 100 Ala RNase T_1 and its specific inhibitor 2′-guanylic acid (2′-GMP) has been refined to $R = 0.186$ using X-ray diffraction data to 1.8-Å resolution. Figure 2 compares the present mutant structure with the equivalent structure of wild-type RNase T_1 complexed with 2′-GMP (Arni et al., 1988). The Phe 100 Ala mutation has only minor effects on the overall structure of the enzyme–inhibitor complex (RMS = 0.29 Å). The most significant change concerns the position of the inhibitor molecule in the active site of the enzyme. The extra space available through the mutation of Phe 100 to alanine is partly occupied by the phosphate group of the inhibitor. The His 92 imidazole moves over 1.3-Å and fills part of the hole, generated by the mutation. The conformation of the His 40 imidazole also changes if compared to wild-type enzyme. In the present X-ray structure, we do not observe any solvent water molecules in the remaining apolar cavity. Single

Table 1. *Steady-state kinetic parameters of wild-type, His 92 Gln, and Phe 100 Ala RNase T_1 for the substrates GpC and GpOMe*

	GpC			GpOMe		
	K_m (K_s)[a] (μM)	k_{cat} (s^{-1})	k_{cat}/K_m ($\mu M^{-1}\ s^{-1}$)	K_m (μM)	k_{cat} (s^{-1})	k_{cat}/K_m ($\mu M^{-1}\ s^{-1}$)
Wild type	216 ± 29 (29.5 ± 3.0)	348 ± 12	1.61 ± 0.22	52 ± 4	$30 \pm 1 \times 10^{-3}$	$5.75 \pm 0.47 \times 10^{-4}$
His 92 Gln	255 ± 32	0.173 ± 0.01	$6.78 \pm 0.91 \times 10^{-4}$	188 ± 42	$1.62 \pm 1 \times 10^{-5}$	$8.62 \pm 2.0 \times 10^{-8}$
Phe 100 Ala	138 ± 13	4.68 ± 0.12	$3.39 \pm 0.33 \times 10^{-2}$	41 ± 5	$4.40 \pm 0.24 \times 10^{-4}$	$1.07 \pm 0.14 \times 10^{-5}$
His 92 Gln + Phe 100 Ala	129 ± 43	20 ± 2	$1.55 \pm 0.54 \times 10^{-5}$	–	–	–

[a] Wild-type reaction obeys Briggs–Haldane kinetics ($K_m > K_s$); the equilibrium dissociation constant has been taken from Steyaert et al. (1991b). For all the other enzyme–substrate complexes, $K_m = K_s$.

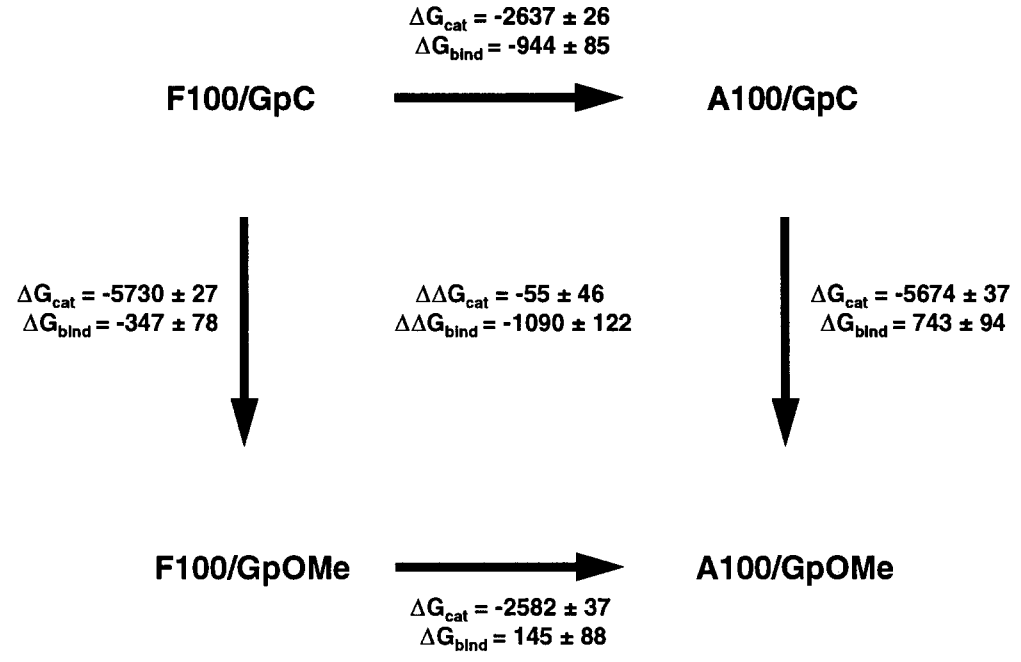

Fig. 1. Thermodynamic cycle to analyze the intermolecular interactions between the Phe 100 side chain and the leaving nucleoside cytidine of the dinucleoside phosphate substrate GpC. ΔG values (cal/mol) equal the the group's apparent contribution to binding if they are calculated from the effect on K_s ($\Delta G_{bind} = +RT \ln(K_s/K_s^{group \to O})$ or the group's apparent contribution to catalysis when derived from the effect on k_{cat} ($\Delta G_{cat} = -RT \ln(k_{cat}/k_{cat}^{group \to O})$.

water molecules indeed have a low tendency to enter apolar cavities (Wolfenden & Radzicka, 1994).

Table 3 compares the intramolecular contacts between the phosphate moiety and the catalytic residues in the present structure with those derived from the wild-type coordinates (Arni et al., 1988). The interactions of the O1P oxygen with Tyr 38 and His 40 appear to be identical in both structures. Movement of the phosphate moiety in the active site, caused by the Phe 100

Table 2. *Crystallization, data collection, data processing, and refinement parameters*

Crystallization conditions	Sitting drop vapor diffusion 10 mg/mL protein, 1.25% (w/v) 2′-GMP, 25 mM NaAc, 2.5 mM $CaAc_2$, pH 4.2
Precipitant	52.5% MPD (v/v)
Space group	$P2_1$
Cell parameters	a = 49.13 Å b = 48.25 Å c = 40.30 Å β = 90.30
Data collection	
Resolution	1.8 Å
Rsym (last resolution shell 1.90–1.82 Å)	0.047 (0.056)
Completeness (last resolution shell 1.90–1.82 Å)	99.7% (100%)
Number of unique reflections used	17,890
Initial model	pdb2aae.ent ($P2_12_12_1$) of Zegers et al. (1992)
Final structure	
Number of water molecules	139
R-factor	0.186
R-free	0.240
Restraints information	
Bond length	0.012 Å
Bond angles	1.835 degrees
Dihedrals	25.8 degrees
Impropers	1.755 degrees

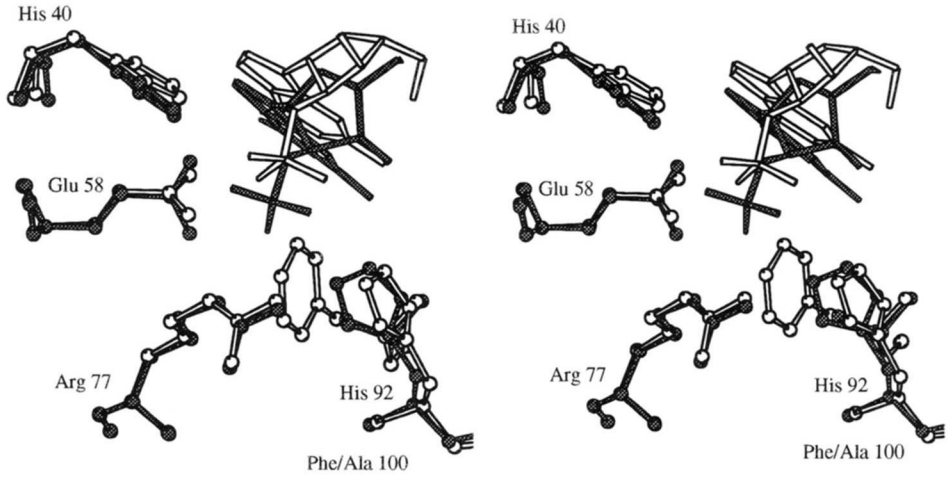

Fig. 2. Stereo view showing the superposition of wild-type (open bonds; Arni et al., 1988) and Phe 100 Ala RNase T_1 (filled bonds) complexed with the specific inhibitor 2′-GMP. Figure generated with the program MOLSCRIPT (Kraulis, 1991).

Ala mutation, generates new or improved contacts between the phosphate moiety with Arg 77 and His 92. In contrast, interactions with the Glu 58 carboxylate appear to be weakened.

Phe 100 exerts its catalytic function independently of the general acid His 92

Apparently, the Phe 100 Ala mutation causes major changes in the intermolecular interactions between the primary site residues Glu 58, Arg 77, and His 92, and the phosphate moiety of the inhibitor 2′-GMP. Therefore, the catalytic defect caused by the Phe 100 Ala mutation may theoretically result indirectly from a change of the interactions between the substrate and other catalytic residues, rather than from a direct interaction between Phe 100 and the substrate in the ES transition-state complex. His 92 has been shown to correspond to the general acid that protonates the leaving group upon expulsion (Heinemann & Saenger, 1982; Steyaert et al., 1990). The prominent structural change in the position of His 92 by the present mutation argues that Phe 100 may be a key residue in maintaining the position of the general acid in the active site. To test this hypothesis, we constructed the double mutant His 92 Gln + Phe 100 Ala RNase T_1 and compared its kinetic parameters to the ones of the corresponding single mutants and wild-type enzyme. The coupling term measures the apparent interaction energy between both residues (Carter et al., 1984; Ackers & Smith, 1985) and is indicative of the functional interactions among the parental residues. The effects of the single His 92 Gln and Phe 100 Ala mutations on substrate turnover (k_{cat}) are additive in the corresponding double mutant (Fig. 3), indicating that both residues contribute to catalysis in an independent way. In contrast to the effect on turnover, we measure significant functional interactions between His 92 and Phe 100 upon substrate binding.

Catalytic function of Phe 100

In the crystal structure of wild-type RNase T_1 complexed with the specific inhibitor 2′-GMP, the Phe 100 phenyl ring makes extensive van der Waals contacts with the nucleotide (Fig. 4A). Both the guanine base and the phosphate moiety of the nucleotide are involved in these contacts. Similar intermolecular interactions between the Phe 100 side chain and the nucleotide are

Table 3. *Comparison of protein–inhibitor contact distances in Phe 100 Ala and wild-type RNase T_1*

	Wild type[a]		Phe 100 Ala[b]		
Inhibitor	Enzyme	Distance (Å)	Enzyme	Mol A (Å)	Mol B (Å)
O1P	His 40Nε2	2.8	His 40Nε2	2.9	3.1
	Tyr 38Oγ	2.7	Tyr 38Oγ	2.7	2.6
O2P	His 92Nε2	4.2	His 92Nε2	3.6	3.5
O3P	Glu 58Oε1	2.7	Glu 58Oε1	2.6	2.6
	Glu 58Oε2	2.4	Glu 58Oε2	3.4	3.2
	Arg 77Nε	4.4	Arg 77Nε	3.1	3.5
	His 92Nε2	4.8	His 92Nε2	2.7	2.8

[a] RNase T_1-2′-GMP (Arni et al., 1988).
[b] Phe 100 Ala RNase T_1-2′-GMP (present paper).

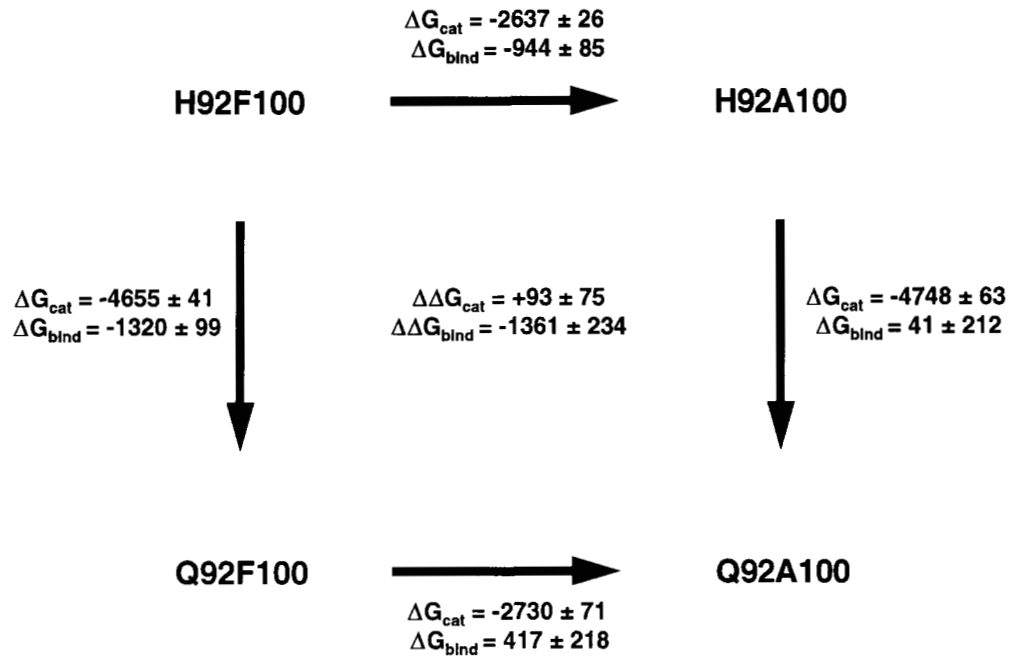

Fig. 3. Thermodynamic cycle to analyze the functional interactions between His 92 and Phe 100 during substrate binding and turnover. ΔG values (cal/mol) equal the the group's apparent contribution to binding if they are calculated from the effect on K_s ($\Delta G_{bind} = +RT\ln(K_s/K_s^{group\rightarrow O})$ or the group's apparent contribution to catalysis when derived from the effect on k_{cat} ($\Delta G_{cat} = -RT\ln(k_{cat}/k_{cat}^{group\rightarrow O})$.

observed in the complexes of RNase T_1 with 3′-GMP (Zegers et al., 1994) and 2′-5′-GpG (Koepke et al., 1989). The observation that the Phe 100 Ala mutation reduces turnover 75-fold strongly suggests that these intermolecular contacts contribute considerably to catalysis.

The catalytic contribution of Phe 100 may result from a direct contact between the Phe 100 aromatic ring and the phosphate moiety of the substrate. The Phe 100 phenyl ring of RNase T_1 is located at the bottom of the catalytic site and is surrounded by the catalytic acid His 92, the catalytic base Glu 58, and Arg 77 (Fig. 5A). These surrounding residues are believed to interact electrostatically with the transition state of the reaction. The apolar Phe 100 side chain may control the dielectric constant of its surroundings, hence enhancing electrostatic interactions between the substrate and the active site. An accurate distribution of polar and apolar side chains in the active site may indeed contribute to stabilizing the charge separations that occur in the transition state because electrons are being redistributed in the process of covalent bond breaking and formation. The hydrophobic side chain of Phe 100 may also disfavor close contacts with (partially) charged oxygen atoms in the ground state, thus accelerating substrate turnover. There is indeed a large change in geometry about the phosphorus as it changes from tetrahedral in the ground state to trigonal bipyramidal in the transition state. It is remarkable to note that the phenyl ring of Phe 8 takes a similar position between the catalytic base His 12 and the catalytic acid His 119 of bovine RNase A, the best known representative of a separate family of eukaryotic ribonucleases (Fig. 5B).

It cannot be excluded that the extensive van der Waals contacts between the Phe 100 side chain and the substrate contribute indirectly to the correct positioning of the pentacovalent phosphorus of the transition state, relative to other catalytic residues (Fig. 4). Indeed, the efficiency of enzyme catalysis depends largely on the precise fit of the transition state in the active site (Knowles, 1991). From a comparison of the crystal structure of wild-type RNase T_1 complexed with 2′-GMP and the corresponding mutant structure (Table 3; Fig. 2 and Kinemage 1), major changes are observed in the intermolecular contact distances between the phosphate moiety and Glu 58, Arg 77, and His 92. Apart from structural adjustments, Phe 100 may also strengthen electrostatic interactions between the enzyme and the substrate. An hydrophobic environment is expected to facilitate electrostatic interactions; the energy of a salt bridge depends strongly on the dielectric constant of the surrounding medium. Our results show that the contribution of Phe 100 to catalysis is independent of the presence of His 92. Unfortunately, we are not able to analyze functional cooperativity of Phe 100 with Glu 58 or Arg 77. So far, we have not been able to purify significant quantities of any recombinant protein mutated at position 77. Most probably, these mutations reduce the stability of the protein to such an extent that proper folding does not occur. pH dependence studies showed that the Glu 58 Ala mutation causes a change in mechanism for the transesterification of the model substrate GpC, catalyzed by RNase T_1 (Steyaert et al., 1990). This change in mechanism makes an analysis of mutual functional interactions between Glu 58 and Phe 100 through double mutant cycles doubtful, if not impossible (Steyaert et al., 1993). We are therefore unable to test if the contribution of the Phe 100 side chain depends on the catalytic residues Glu 58 or Arg 77 by constructing the corresponding double mutant cycles.

It is well established that polar groups in the active sites of many enzymes act as acid or base or simply stabilize the transition state electrostatically. The present results lead to the con-

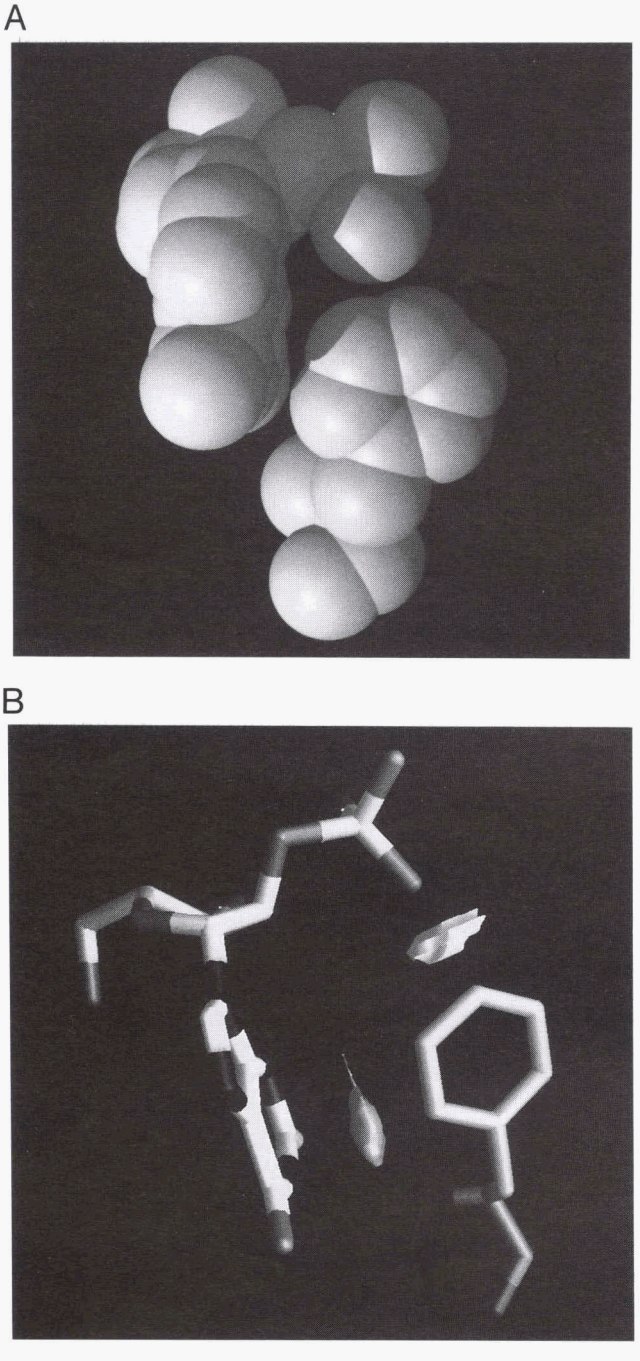

Fig. 4. Effect of the Phe 100 Ala mutation on the binding of the specific inhibitor 2′-GMP to RNase T_1. **A:** van der Waals interactions between Phe 100 and the specific inhibitor 2′-GMP in the wild-type RNase T_1-2′-GMP complex (Arni et al., 1988). **B:** van der Waals clashes between 2′-GMP of the present Phe 100 Ala mutant structure superimposed on wild-type RNase T_1 (Arni et al., 1988). Figures generated with the programs Raster3D (Merritt & Murphy, 1994) and GRASP (Nicholls et al., 1993).

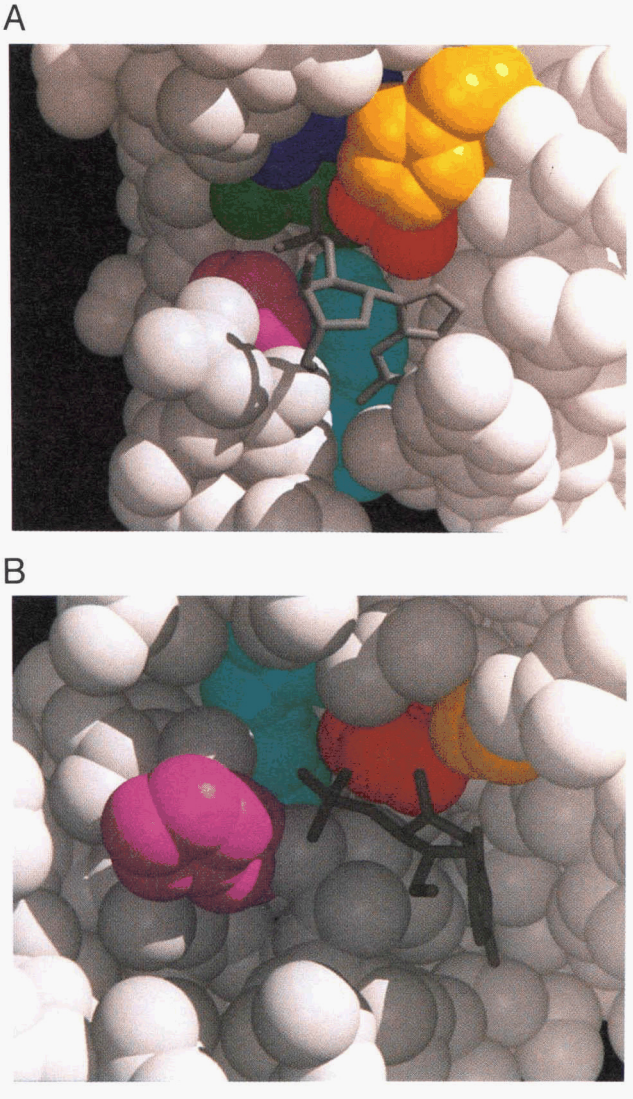

Fig. 5. CPK and ball-and-stick representation of the active site of (**A**) wild-type RNase T_1 complexed with the specific inhibitor 2′-GMP (Arni et al., 1988) and (**B**) bovine RNase A with 3′-CMP (Zegers et al., 1994). RNase T_1/RNase A: cyan, Phe 100/Phe 8; yellow, His 40/Lys 41; magenta, His 92/His 119; red, Glu 58/His 12; blue, Tyr 38; green, Arg 77. Figure generated with the program Raster3D (Merritt & Murphy, 1994).

clusion that apolar residues may also contribute considerably to catalyzing conversions of charged molecules to charged products, involving even more polar transition states. Indeed, a second negative charge develops on the pentacovalent phosphate transition state of the ribonuclease catalyzed reaction (Eckstein et al., 1972).

Materials and methods

Construction and purification of RNase T_1 mutants

The preparation and purification of wild-type RNase T_1 and the mutant His 92 Gln have been reported previously (Steyaert et al., 1990). The Phe 100 Ala single mutant and the His 92 Gln + Phe 100 Ala double mutant were constructed by oligonucleotide-directed mutagenesis (Stanssens et al., 1989) using the primers 5′-GCACCAGTCTGAGTG-3′ (His 92 Gln) and 5′-GTACATTCAACGCGTTGTTACC-3′ (Phe 100 Ala).

Enzymes were purified to homogeneity as described (Steyaert et al., 1990).

Kinetic procedures

All kinetics were performed at 35 °C in a buffer containing 50 mM imidazole, 50 mM NaCl, and 2.5 mM EDTA at pH 6.0 (ionic strength = 0.1 M). RNase T_1 concentrations are based on $A_{278nm} = 1.54$ for a 0.1% solution (Shirley & Laurents, 1990). The values and standard errors of the kinetic parameters were obtained from nonlinear least-squares analysis using the program ENZFITTER (Leatherbarrow, 1987).

The steady-state kinetic parameters for the conversion of GpC to cGMP and C by Phe 100 Ala and His 92 Gln + Phe 100 Ala RNase T_1 were determined from initial velocities by measuring the increase in absorbency at 280 nm (Zabinski & Walz, 1976) as described (Steyaert et al., 1991a). The parameters for wild-type and His 92 Gln RNase T_1 were taken from Steyaert et al. (1991a).

The steady-state kinetic constants k_{cat} and K_m for the Phe 100 Ala RNase T_1-catalyzed transesterification of the synthetic substrate GpOMe were determined from initial velocity measurements as described (Steyaert et al., 1991a). The data on wild-type RNase T_1 and His 92 Gln RNase T_1 were taken from Steyaert et al. (1991a).

Crystallization and data collection

Co-crystals of Phe 100 Ala RNase and the specific inhibitor 2′-GMP were obtained with the sitting drop vapor diffusion method using macroseeding. A solution of 10 mg/mL recombinant Phe 100 Ala RNase T_1 and 1.25% (w/v) 2′-GMP in 25 mM sodium acetate and 2.5 mM calcium acetate at pH 4.2 was equilibrated against 52.5% MPD. Small, well-formed microcrystals of wild-type RNase T_1 (grown under the same conditions) were used as seeds in the sitting drop experiments. Intensity data were collected on a large MAR image plate and processed using the CCP4 suite of programs (CCP4, 1994).

Structural refinement of Phe 100 Ala RNase T_1

We used the coordinates of the P*21* His 40 Lys RNase T_1 structure (Zegers et al., 1992) as a near-isomorphous model for solving the structure of the Phe 100 Ala mutant. The space group and cell constants of the mutant under investigation were found to be very similar to the ones of our base model. After removal of all non-protein atoms and the Lys 40 and Phe 100 side chains, molecular replacement was performed using the program Amore (Navaza, 1994). The resulting solution gave an R-factor of 0.369. Successive sessions of stereochemically restrained least-squares refinements using X-PLOR (Brünger, 1992) and manual model revisions using the graphics program O (Jones et al., 1991) on an SGI Indigo were performed, leading us to the final refined structure with an R-factor of 0.186 and an R_{free} of 0.240. The His 40 side chain was manually fitted into the difference electron density maps after the first couple of refinement cycles. Because of the orthorhombic pseudosymmetry of the data, a significant correlation exists between the two octants of the X-ray data, thus reducing the number of independently observed data points. Therefore, we used noncrystallographic symmetry restrains between the two molecules in the asymmetric unit throughout the refinement. The refined model coordinates have been deposited in the Brookhaven Data Bank (accession number: pdb1bir.ent).

Acknowledgments

We acknowledge the support of Rex Palmer and John Cooper (Birbeck College, London, UK) with data collection. M.G. was supported by an E.C. *Tempus* fellowship. I.Z. and R.L. are senior research assistants of the Belgian Fund for Scientific Research.

References

Ackers GK, Smith FR. 1985. Effects of site-specific amino acid modifications on protein interactions and biological function. *Annu Rev Biochem 54*:597–629.

Arni R, Heinemann U, Tokuoka R, Saenger W. 1988. Three-dimensional structure of the ribonuclease T_1^*2'-GMP complex at 1.9 Å resolution. *J Biol Chem 263*:15358–15368.

Brünger AT. 1992. *X-PLOR version 3.1: A system for crystallography and NMR*. New Haven, Connecticut: Yale University.

Carter PJ, Winter G, Wilkinson AJ, Fersht AR. 1984. The use of double mutants to detect structural changes in the active site of tyrosyl-tRNA synthetase (*Bacillus stearothermophilus*) *Cell 36*:835–840.

CCP4. 1994. Collaborative Computational Project, Number 4. The CCP4 suite: Programs for protein crystallography. *Acta Crystallogr D 50*: 760–763.

Eckstein F, Schulz HH, Rüterjans H, Haar W, Maurer W. 1972. Stereochemistry of the transesterification step of ribonuclease T_1. *Biochemistry 11*:3507–3512.

Fersht AR. 1988. Relationships between apparent binding energies measured in site-directed mutagenesis experiments and energetics of binding and catalysis. *Biochemistry 27*:1577–1580.

Grunert HP, Zouni A, Beineke M, Quaas R, Georgalis Y, Saenger W, Hahn U. 1991. Studies on RNase T_1 mutants affecting enzyme catalysis. *Eur J Biochem 197*:203–207.

Heinemann U, Saenger W. 1982. Specific protein-nucleic acid recognition in Ribonuclease T_1-guanilic acid complex: An X-ray study. *Nature 299*: 27–31.

Hill C, Dodson G, Heinemann U, Saenger W, Mitsui Y, Nakamura K, Borisov SG, Polyakov K, Pavlovsky S. 1983. The structural and sequence homology of a family of microbial ribonucleases. *Trends Biochem Sci 8*:364–369.

Jones TA, Zou JY, Cowan SW, Kjeldgaard M. 1991. Improved methods for building protein models in electron density maps and the location of errors in these models. *Acta Crystallogr A 47*:110–119.

Knowles J. 1991. Enzyme catalysis: Not different, just better. *Nature 350*: 121–124.

Koepke J, Maslowska M, Heinemann U, Saenger W. 1989. Three-dimensional structure of ribonuclease T_1 complexed with guanylyl-2′,5′-guanosine at 1.8 Å resolution. *J Mol Biol 206*:475–488.

Kraulis P. 1991. MOLSCRIPT: A program to produce both detailed and schematic plots of proteins. *J Appl Crystallogr 24*:946–950.

Leatherbarrow R. 1987. *ENZFITTER*. Cambridge, UK: Biosoft, Hills Road.

Meiering EM, Serrano L, Fersht AR. 1992. Effect of active site residues in Barnase on activity and stability. *J Mol Biol 225*:585–589.

Merritt EA, Murphy MEP. 1994. Raster 3D version 2.0—A program for photorealistic molecular graphics. *Acta Crystallogr D 50*:869–873.

Navaza J. 1994. *AMoRe*: An automated package for molecular replacement. *Acta Crystallogr A 50*:157–163.

Nicholls A, Sharp KA, Honig B. 1993. Protein folding and association: Insights from the interfacial and thermodynamic properties of hydrocarbons. *Proteins Struct Funct Genet 11*:281–296.

Nishikawa S, Morioka H, Kim HJ, Fuchimura K, Tanaka T, Uesugi S, Hakoshima T, Tomita K, Ohtsuka E, Ikehara M. 1987. Two histidines are essential for Ribonuclease T_1 activity as is the case for ribonuclease A. *Biochemistry 26*:8620–8624.

Poteete AR, Rennell D, Bouvier SE. 1992. Functional significance of conserved amino acid residues. *Proteins Struct Funct Genet 13*:38–40.

Shirley BA, Laurents DL. 1990. Purification of recombinant ribonuclease T_1 expressed in *Escherichia coli*. *J Biochem Biophys Met 20*:181–188.

Stanssens P, Opsomer C, McKeown YM, Kramer W, Zabeau M, Fritz HJ. 1989. Efficient oligonucleotide-directed construction of mutations in expression vectors by the gapped duplex DNA method using alternating selectable markers. *Nucleic Acids Res 17*:4441–4454.

Steyaert J, Haikal AF, Wyns L, Stanssens P. 1991a. Subsite interactions of Ribonuclease T_1: Asn 36 and Asn 98 accelerate GpN transesterification through interactions with the leaving nucleoside N. *Biochemistry 30*: 8666–8670.

Steyaert J, Hallenga K, Wyns L, Stanssens P. 1990. Histidine-40 of ribonuclease T_1 acts as base catalyst when the true catalytic base, Glutamic acid-58, is replaced by alanine. *Biochemistry 29*:9064–9072.

Steyaert J, Wyns L. 1993. Functional interactions among the His40, Glu58 and His92 catalysts of Ribonuclease T_1 as studied by double and triple mutants. *J Mol Biol 229*:770–781.

Steyaert J, Wyns L, Stanssens P. 1991b. Subsite interactions of Ribonuclease T_1: Viscosity effects indicate that the rate limiting step of GpN transesterification depends on the nature of N. *Biochemistry 30*:8661–8665.

Wolfenden R, Radzicka A. 1994. On the probability of finding a water molecule in a nonpolar cavity. *Science 265*:936–937.

Zabinski M, Walz F. 1976. Subsites and catalytic mechanism of Ribonuclease T_1: Kinetic studies using GpC and GpU as substrates. *Arch Biochem Biophys 175*:558–564.

Zegers I, Maes D, Dao-Thi MH, Poortmans F, Palmer R, Wyns L. 1994. The structures of RNase A with 3′-CMP and d(CpA): Active site conformation and conserved water molecules. *Protein Sci 3*:2322–2339.

Zegers I, Verhelst P, Choe HW, Steyaert J, Heinemann U, Saenger W, Wyns L. 1992. Role of histidine-40 in ribonuclease T_1 catalysis: Three-dimensional structures of the partially active His 40 Lys mutant. *Biochemistry 31*:11317–11325.